RADIOISOTOPES, **50**, 463–471 (2001)

Information

Diagonal Elements Fitting Technique to Improve Response Matrixes for Environmental Gamma Ray Spectrum Unfolding

Susumu MINATO [*1]

[*1] Seto Site, Chubu Center of the National Institute of Advanced Industrial Science and Technology
110 Nishiibara-machi, Seto-shi, Aichi Pref. 489-0884, Japan

Key Words : environmental gamma ray, response matrix, spectrum unfolding, uranium, thorium, potassium

1. Introduction

An original response matrix for terrestrial gamma ray spectrum unfolding was derived in 1970[1] to evaluate the exposure rates. Since then, some improvements have been made to obtain not only the exposure rate but also many more pieces of information about terrestrial gamma ray fields such as effective dose rate, concentrations of potassium (K), uranium (U) and thorium (Th) in the environment and discrimination between natural and man-made contributions[2].

In this paper, standard response matrixes are reevaluated for various sizes of NaI(Tl) scintillators so that a more precision spectrum unfolding can be done. In addition, parameters required to evaluate the concentrations of K, U and Th are also updated.

In order to evaluate the quantities just mentioned as accurately as possible, we have to prepare a response matrix tailored to the performance of individual scintillators. This paper proposes a diagonal elements fitting (DEF) technique. From the standard response matrix, this technique enables us to reproduce a new matrix easily and quickly matching the resolution for a scintillator used for measurement.

環境γ線スペクトルアンフォールディング用応答行列改良のための対角要素適合技術。湊　進：産業技術総合研究所中部センター瀬戸サイト，489-0884　愛知県瀬戸市西茨町 110。

2. Outline of the Response Matrix Method

2・1 Principle

The spectrum unfolding[3] is carried out based on the relationship between a measured pulse height distribution, $P(V)$, and an incident gamma ray energy spectrum, $N(E)$,

$$P(V)=\int_0^\infty R(V,E)N(E)\mathrm{d}E \qquad (1)$$

where $R(V,E)$ is the response function of the detector.

Since pulse height distributions are measurable at a set of discrete energy bins, Eq.(1) can be replaced by a matrix equation

$$Pi=\sum_{j=1}^{n} R_{ij}N_j, \qquad i=1,2,\ldots,n. \qquad (2)$$

By solving Eq.(2), we obtain the incident gamma ray energy spectrum, N_j.

The matrix elements are approximately expressed as:

$$R_{ij}=\int_{V_i-\Delta V_i/2}^{V_i+\Delta V_i/2} R(V,E_j)\,\mathrm{d}V. \qquad (3)$$

Here, ΔV_i is the pulse height interval. Since we usually derive a square matrix, ΔV_i is equal to ΔE_i, the

energy interval in the i-th energy bin. The value of E_j in Eq.(3) is chosen to be a central value in each interval.

2·2 Energy bin

The division of the energy range is determined so that the photo-peaks due to 1.464 MeV gamma rays emitted from ^{40}K, 1.765 and 2.205 MeV from ^{214}Bi (U-series) and 2.615 MeV from ^{208}Tl (Th-series) may be included in a single bin, respectively. Furthermore, the energy interval is set as nearly equal as the full width at half maximum for each photo-peak. Table 1 gives the energy intervals for the bins determined in the way mentioned above. The bin number 14 corresponds to ^{40}K peak, 16 and 18 to ^{214}Bi and 20 to ^{208}Tl, respectively.

2·3 The response matrix

Tables 2-4 give 22×22 matrixes for different types of NaI(Tl) scintillators for an isotropic field, since it is known that the flux density and the dose rate per unit solid angle are almost isotropic in the natural environment[4]. The calculations were done using a Monte Carlo code, SPHERIX[5]. A total of 1 000 000 histories were traced per each incident energy. The resolution R for ^{40}K and the power index q given in the table captions will be described in detail in a later section.

2·4 Unfolding

From Eq.(2), the incident gamma ray spectrum can be determined by one of several unfolding methods[3]. Here, we give an iterative method as an example.

Table 1 Basic quantities to evaluate dose rate and K, U and Th concentrations

Bin No.	Energy (MeV)	μ_{en}/ρ of air ($cm^2 \cdot g^{-1}$)	Cosmic ray count rate*	Flux density ($cm^{-2} \cdot MeV^{-1} \cdot s^{-1}$)		
				1% K	1 ppm U	1 ppm Th
01	0.050-0.150	0.0234	15.0	5.47	4.32	2.12
02	0.150-0.250	0.0268	7.5	2.15	1.59	0.753
03	0.250-0.350	0.0288	4.9	1.09	0.892	0.340
04	0.350-0.450	0.0295	3.1	0.647	0.412	0.168
05	0.450-0.550	0.0297	2.3	0.471	0.244	0.154
06	0.550-0.650	0.0296	1.7	0.397	0.467	0.136
07	0.650-0.750	0.0293	1.3	0.321	0.166	0.0875
08	0.750-0.850	0.0289	1.0	0.266	0.137	0.0797
09	0.850-0.950	0.0285	0.88	0.272	0.0887	0.141
10	0.950-1.050	0.0280	0.70	0.253	0.0777	0.101
11	1.050-1.150	0.0275	0.60	0.257	0.171	0.0153
12	1.150-1.250	0.0271	0.50	0.218	0.126	0.0128
13	1.250-1.390	0.0265	0.40	0.268	0.0990	0.0124
14	1.390-1.540	0.0258	0.37	2.13	0.0752	0.0212
15	1.540-1.690	0.0253	0.28		0.0516	0.0401
16	1.690-1.840	0.0246	0.24		0.170	0.00972
17	1.840-2.100	0.0239	0.19		0.0129	0.00540
18	2.100-2.310	0.0232	0.16		0.0382	0.00756
19	2.310-2.510	0.0227	0.13		0.00825	0.00664
20	2.510-2.720	0.0221	0.12		0.00156	0.0901
21	2.720-3.000	0.0215	0.10			
22	3.000-3.200	0.0210	0.090			

* counts/s per MeV for a 3" ϕ spherical NaI(Tl)

Table 2 Response matrix for 3"ϕ × 3" NaI(Tl) in isotropic field: R=7.0(%), q=0.34

	01	02	03	04	05	06	07	08	09	10	11	12	13	14	15	16	17	18	19	20	21	22
01	66.73																					
02	1.95	60.02																				
03	4.65	1.04	50.07																			
04	4.88	4.97	0.26	40.89																		
05	4.71	4.49	4.52	0.19	33.98	0.01																
06	4.18	4.06	4.24	3.92	0.22	29.05	0.07															
07	3.60	3.60	3.70	4.01	3.40	0.34	25.12	0.20														
08	3.11	3.14	3.16	3.37	3.88	3.01	0.53	21.99	0.40													
09	2.68	2.70	2.72	2.88	3.15	3.75	2.69	0.77	19.31	0.64												
10	2.35	2.34	2.38	2.46	2.65	2.97	3.61	2.38	0.97	17.14	0.88											
11	2.06	2.07	2.08	2.12	2.25	2.47	2.84	3.43	2.15	1.20	15.26	1.10										
12	1.83	1.83	1.84	1.90	1.95	2.10	2.35	2.73	3.29	1.90	1.41	13.63	1.34									
13	1.63	1.61	1.61	1.63	1.67	1.76	1.92	2.16	2.50	3.02	2.24	0.81	13.95	0.58								
14	1.39	1.38	1.39	1.38	1.42	1.47	1.56	1.71	1.90	2.21	2.61	2.76	1.44	12.74	0.60							
15	1.20	1.18	1.19	1.21	1.22	1.48	1.34	1.40	1.52	1.69	2.15	2.28	3.66	1.74	11.37	0.76						
16	1.03	1.03	1.04	1.04	1.05	1.08	1.30	1.31	1.28	1.37	1.45	1.82	3.08	3.64	1.84	10.15	0.93					
17	0.86	0.87	0.86	0.86	0.88	0.89	0.91	0.94	1.23	1.36	1.22	1.27	1.96	3.17	3.41	2.09	10.84	0.15				
18	0.71	0.71	0.71	0.72	0.73	0.72	0.74	0.75	0.77	0.81	0.94	1.49	1.60	1.84	2.51	3.27	4.23	9.07	0.57			
19	0.61	0.61	0.61	0.61	0.62	0.63	0.65	0.63	0.65	0.67	0.69	0.72	1.53	1.95	1.71	2.04	5.50	3.08	8.03	0.78		
20	0.53	0.53	0.54	0.52	0.53	0.55	0.53	0.54	0.56	0.56	0.59	0.60	0.89	1.18	2.21	1.66	3.77	4.42	2.90	7.48	0.80	
21	0.47	0.46	0.45	0.45	0.45	0.46	0.46	0.47	0.47	0.48	0.49	0.50	0.71	0.82	0.90	1.66	3.25	2.87	4.29	3.12	7.89	0.44
22	0.39	0.40	0.39	0.38	0.40	0.39	0.40	0.39	0.40	0.41	0.42	0.41	0.62	0.69	0.72	0.76	2.58	2.64	2.47	4.53	4.38	5.92

We set $N_j^{(1)}$, the first order approximation to N_j, equal to the observed pulse height distribution $P_j^{(0)}$, namely, $N_j^{(1)}=P_j^{(0)}$. Next, we set $P_i^{(1)}$, the first order approximation to P_i, as follows:

$$P_i^{(1)}=\sum_{j=1}^{n} R_{ij}N_j^{(1)}. \tag{4}$$

In general,

$$P_i^{(k)}=\sum_{j=1}^{n} R_{ij}N_j^{(k)}. \tag{5}$$

The j-th element of the k+1 approximation of the spectrum $N_j^{(k+1)}$ is given as follows:

$$N_j^{(k+1)}=\frac{N_j^{(k)}}{P_i^{(k)}}P_j^{(0)} \tag{6}$$

The iterative cycle is repeated until the series of trial vector $N^{(k)}$ achieves a satisfactory degree of convergence. A cycle of 20 is chosen in this paper.

Figure 1 shows an example of a measured pulse height distribution. The peak search was made for ^{40}K and ^{208}Tl photo-peaks for energy calibration to allot the counts into each energy bin. To determine the peak positions by smoothing the distribution, we took the first 20 terms, i.e., n_{max}=20, of the coefficients in Fourier expansion.

Next, a cosmic ray contribution[6] was subtracted from the pulse height distribution using Table 1 by normalizing at the energy bin 22. The cosmic ray count rate values given in Table 1 are only for a 3"ϕ spherical scintillator. We, however, use this shape for the other types of scintillators also as an approximation. Moreover, a ^{40}K contamination contribution due to a photo-multiplier tube should be subtracted in advance[7].

The observed spectrum shown in Fig. 2 is the resultant unfolded flux density, Φ_j, where

Table 3 Response matrix for 2"$\phi \times 2$" NaI(Tl) in isotropic field: R=7.0(%), q=0.45

	01	02	03	04	05	06	07	08	09	10	11	12	13	14	15	16	17	18	19	20	21	22
01	29.48																					
02	0.90	25.29																				
03	2.37	0.47	19.08																			
04	2.54	2.30	0.12	14.24																		
05	2.36	2.11	2.02	0.08	11.07																	
06	1.98	1.87	1.89	1.74	0.09	8.98	0.02															
07	1.66	1.61	1.63	1.75	1.46	0.12	7.45	0.06														
08	1.39	1.36	1.38	1.44	1.64	1.27	0.17	6.33	0.11													
09	1.18	1.15	1.15	1.19	1.32	1.56	1.12	0.23	5.44	0.18												
10	1.02	0.99	1.01	1.01	1.06	1.22	1.48	0.98	0.29	4.70	0.24											
11	0.88	0.86	0.87	0.89	0.91	0.99	1.16	1.39	0.88	0.35	4.12	0.30										
12	0.78	0.77	0.76	0.78	0.78	0.84	0.93	1.08	1.31	0.76	0.40	3.64	0.36									
13	0.67	0.66	0.65	0.65	0.68	0.68	0.76	0.85	0.99	1.18	0.90	0.25	3.67	0.15								
14	0.57	0.57	0.57	0.55	0.58	0.58	0.61	0.66	0.72	0.85	1.03	1.09	0.49	3.28	0.16							
15	0.49	0.48	0.48	0.47	0.48	0.60	0.52	0.55	0.58	0.64	0.80	0.86	1.42	0.58	2.90	0.20						
16	0.42	0.42	0.42	0.41	0.41	0.43	0.52	0.51	0.49	0.54	0.56	0.68	1.14	1.40	0.60	2.55	0.23					
17	0.34	0.34	0.34	0.34	0.35	0.35	0.36	0.36	0.50	0.53	0.46	0.49	0.75	1.14	1.29	0.78	2.68	0.04				
18	0.28	0.28	0.28	0.29	0.28	0.29	0.29	0.30	0.30	0.30	0.37	0.62	0.61	0.69	0.90	1.17	1.52	2.20	0.14			
19	0.24	0.24	0.24	0.23	0.24	0.24	0.25	0.25	0.25	0.26	0.26	0.27	0.62	0.77	0.63	0.74	1.93	1.06	1.93	0.19		
20	0.21	0.20	0.21	0.20	0.21	0.21	0.21	0.22	0.21	0.22	0.23	0.23	0.33	0.45	0.92	0.62	1.36	1.53	0.96	1.78	0.19	
21	0.18	0.18	0.17	0.18	0.17	0.17	0.17	0.18	0.18	0.18	0.19	0.19	0.27	0.31	0.33	0.68	1.29	1.04	1.44	1.07	1.88	0.10
22	0.15	0.15	0.15	0.15	0.15	0.15	0.15	0.15	0.16	0.15	0.16	0.17	0.23	0.26	0.27	0.29	1.04	1.05	0.90	1.51	1.43	1.38

$$\Phi_j = \frac{N_j}{\Delta E_j}, \quad j = 1, 2, \ldots, 22 \qquad (7)$$

The description of the theoretical spectrum shown in the figure will be given in a later section.

3. Evaluation of Potassium, Uranium and Thorium Concentrations

Figure 2 reveals the clear peaks due to ^{40}K (Bin No. 14), ^{214}Bi (Nos. 16 and 18) and ^{208}Tl (No. 20). From the intensities of the peaks, we can estimate the concentrations of K, U and Th by comparing with theoretically evaluated flux density spectra due to these nuclides. The flux density spectra used so far were computed by assuming the soil to be aluminum based on relatively old nuclear data[2), 4), 8)]. In this study, therefore, we reevaluate the flux densities using a new model.

The flux densities in these bins consist of primary (unscattered) components due to ^{40}K, U-, and Th-series and scattered components caused by the primaries. In the first place, therefore, we have to calculate these components for unit concentrations of K, U and Th in the environment. To do this, we assume the K, U and Th sources to be uniformly distributed in the ground with infinite half-space geometry. The composition of the soil is assumed to be SiO_2 alone as an approximation. Its bulk density is, however, chosen to be 1.6 g/cm^3. The density of air is taken to be 1.205 mg/cm^3. We use a gamma ray transport calculation code to obtain the flux densities at 1 m above the ground.

Since the primary components consist of discrete line spectra, these have to be assigned appropriately to the respective energy bins. We characterize by the

Table 4 Response matrix for 3"ϕ spherical NaI(Tl) in isotropic field: R=7.0(%), q=0.40

	01	02	03	04	05	06	07	08	09	10	11	12	13	14	15	16	17	18	19	20	21	22
01	45.24																					
02	1.33	42.28																				
03	3.31	0.72	35.56																			
04	3.62	3.56	0.18	28.77																		
05	3.53	3.26	3.19	0.13	23.65	0.01																
06	3.09	3.01	3.08	2.82	0.15	20.00	0.05															
07	2.68	2.68	2.69	2.93	2.45	0.24	17.16	0.14														
08	2.28	2.31	2.34	2.48	2.83	2.16	0.36	14.86	0.28													
09	1.95	1.98	2.02	2.10	2.28	2.71	1.87	0.50	13.01	0.44												
10	1.69	1.73	1.75	1.82	1.92	2.13	2.59	1.70	0.67	11.48	0.60											
11	1.49	1.50	1.53	1.57	1.66	1.78	2.05	2.47	1.53	0.81	10.16	0.75										
12	1.32	1.33	1.35	1.38	1.44	1.53	1.67	1.97	2.35	1.36	0.94	9.08	0.88									
13	1.17	1.15	1.17	1.21	1.22	1.28	1.38	1.55	1.81	2.17	1.59	0.54	9.22	0.37								
14	0.99	1.00	1.02	1.02	1.07	1.09	1.18	1.23	1.34	1.55	1.85	1.99	0.96	8.35	0.38							
15	0.86	0.85	0.86	0.85	0.90	1.07	0.97	1.03	1.11	1.18	1.49	1.63	2.63	1.19	7.42	0.50						
16	0.74	0.73	0.75	0.76	0.75	0.78	0.95	0.95	0.93	0.98	1.05	1.29	2.19	2.62	1.24	6.63	0.60					
17	0.61	0.62	0.62	0.62	0.63	0.64	0.65	0.68	0.91	0.97	0.85	0.91	1.41	2.22	2.45	1.42	7.04	0.10				
18	0.50	0.51	0.51	0.51	0.52	0.52	0.54	0.55	0.56	0.57	0.70	1.11	1.15	1.32	1.74	2.32	2.94	5.86	0.36			
19	0.44	0.44	0.45	0.44	0.43	0.46	0.46	0.46	0.48	0.49	0.50	0.51	1.10	1.41	1.22	1.42	3.85	2.11	5.19	0.50		
20	0.37	0.37	0.39	0.38	0.38	0.38	0.40	0.40	0.40	0.41	0.42	0.44	0.64	0.85	1.61	1.17	2.62	3.09	1.97	4.82	0.51	
21	0.33	0.32	0.32	0.32	0.32	0.32	0.33	0.34	0.35	0.34	0.35	0.36	0.52	0.60	0.65	1.20	2.32	2.00	2.99	2.15	5.05	0.27
22	0.28	0.27	0.27	0.28	0.28	0.28	0.28	0.29	0.30	0.30	0.30	0.31	0.44	0.49	0.52	0.56	1.85	1.88	1.74	3.11	3.01	3.79

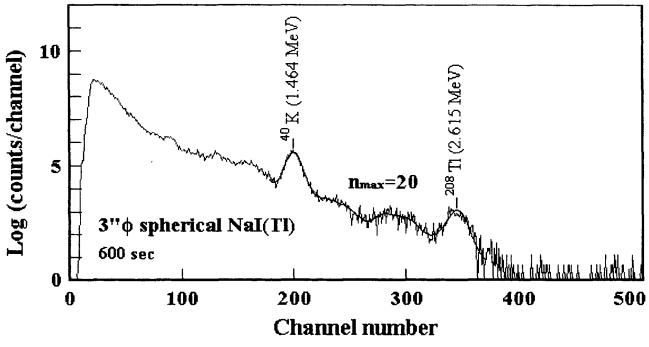

Fig. 1 Pulse height distribution.

suffix m the energies of primary gamma rays emitted from K, U- and Th-series. In addition, we denote the central value of each energy bin by E_j. Then, the assignment of the primary components can be made from the following formulas.

$$N_{j-1}^{P} = \frac{E_i - E_m}{E_j - E_{j-1}} N_m^P \ ,$$

$$N_j^P = \frac{E_m - E_{j-1}}{E_j - E_{j-1}} N_m^P \ . \qquad (8)$$

In Table 1, the calculated results for the primary

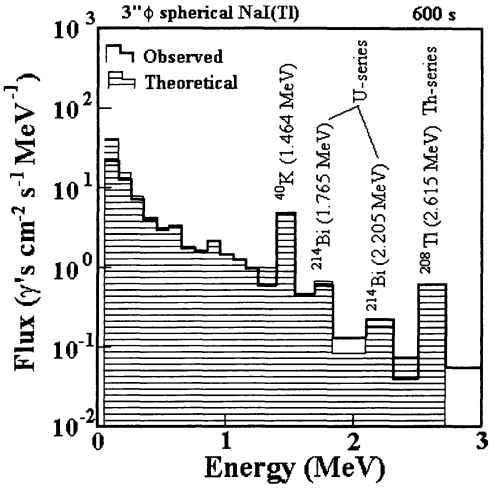

Fig. 2 Unfolded spectrum of the pulse height distribution shown in Fig.1.

Table 5 A 3×3 matrix to evaluate K, U and Th concentrations

	$K(V_{14})$	$U(V_{16,18})$	$Th(V_{20})$
$K(E_{14})$	0.320		
$U(E_{16,18})$	0.0113	0.0335	0.000327
$Th(E_{20})$	0.00318	0.00305	0.0189

plus scattered components are presented for unit concentrations of K, U and Th in the soil. The calculations were done using a Monte Carlo code, MONARIZA/G2[8]. A total of 1 000 000 histories were traced for K, U and Th, respectively. The data of emission energies and disintegration rates were taken from Beck[9] and Beck et al.[10].

The concentrations of K, U and Th are calculated from the values of N_{14}, $N_{16}+N_{18}$ and N_{20} by the iterative method through the 3×3 matrix given in Table 5, which was derived by multiplying the corresponding flux density given in Table 1 by the energy interval of each energy bin.

4. Diagonal Elements Fitting (DEF)

Originally, the response matrix method was developed to analyze continuous spectra. However, for a spectrum including both continuous and discrete components like an environmental gamma ray spectrum, the response matrix with sufficient precision has to be used for unfolding. Otherwise, it can lead to large oscillations in the energy bins adjacent to the peaks of K, U and Th.

Although Tables 2-4 are for a resolution for K photo-peak to be 7 %, there are a wide variety of commercially available scintillators in resolution. In other words, every detector resolution is different from one another. The Monte Carlo method is too time-consuming to recalculate the response matrix fitted to every resolution of detectors. The technique of DEF enables us to reconstruct a new matrix easily and quickly from the standard response matrix.

4·1 Determination of the resolution function

It is well known that the photo-peak can be closely approximated by a Gaussian whose mean value is proportional to an incident energy E and whose standard deviation $\sigma(E)$ must be obtained from experimental data. The resolution of the detector is defined to be the ratio

$$r(E) = \frac{W(E)}{E} \times 100 \quad (\%) , \tag{9}$$

where W is the full width at half maximum of the Gaussian, i.e.,

$$W = 2\sigma\sqrt{2\ln 2.} \tag{10}$$

The energy dependence of the detector resolution can be expressed by a power law,

$$r(E) = r(E^*)\left(\frac{E^*}{E}\right)^q , \tag{11}$$

where E^* is a reference energy which we take to be the energy of ^{40}K gamma rays (1.464 MeV) in this study. The power index q is usually taken to be 0.34 for 3"ϕ×3" NaI(Tl)[11]. For 2"ϕ×2", and 3" ϕ spherical NaI(Tl), we adopt the value of q=0.45 and 0.40, respectively, which were determined by experiments in this work.

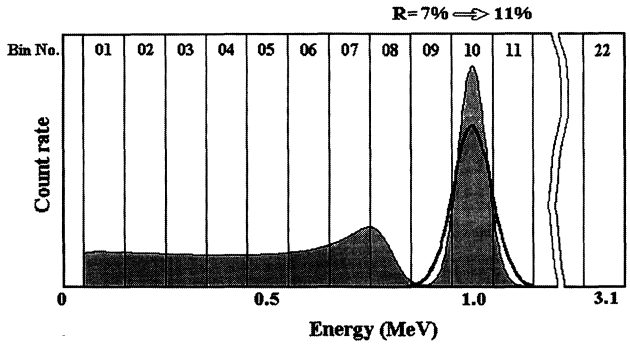

Fig. 3 Comparison between the original and the broadened photo-peaks.

4·2 Correction for the diagonal and the neighboring elements

We explain here how to modify the matrix elements referring to the row 10 of a matrix as an example (See Fig. 3). Let us assume that the resolution for ^{40}K photo-peak of the detector used amounts to R=11%. The new matrix elements for the energy bins 09, 10 and 11 can be calculated in accordance with the Gaussian distribution using Eqs. (9)-(11). We replace the old values in these bins with the new elements. It should be noted that, in the bin 09, a Compton edge is included in addition to the photo-peak component. The Compton component is evaluated, in advance, by subtracting the count in the bin 11 from that in 09. All the diagonal elements and the neighbors are replaced in the manner just mentioned.

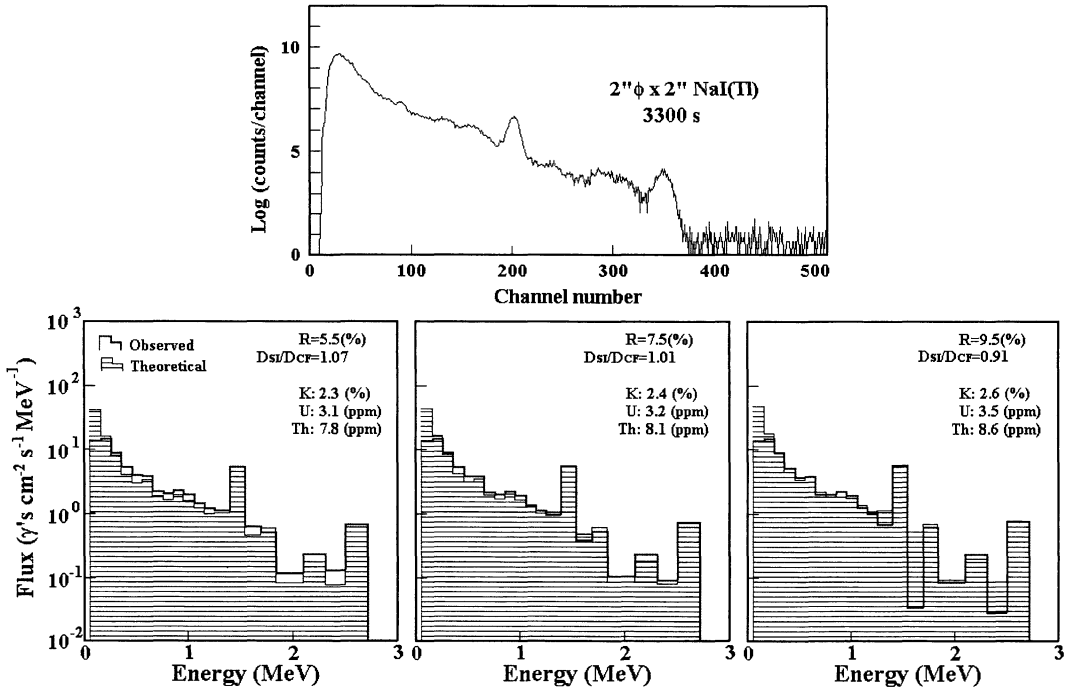

Fig. 4 Comparison among three spectra unfolded by different resolutions.

The full description of the procedure mentioned above and its calculation code is given in Ref.12.

5. Example of Application

Figure 4 shows the spectra unfolded from a single pulse height distribution given at the upper part in the figure for the three different values of resolution for ^{40}K photo-peak. The concentrations of K, U and Th were estimated using Table 5. The theoretical spectrum was obtained by multiplying the flux density per unit concentration in Table 1 by the respective concentration values estimated above.

The absorbed dose rate in air is calculated from the following two methods. One is from a spectral integration of the unfolded spectrum.

$$D_{SI} = G_V \sum_{j=1}^{22} E_j (\mu_{en}/\rho)_j \Phi_j \Delta E_j . \qquad (12)$$

Here, D_{SI} is the dose rate, E_j is the incident gamma ray energy, Φ_j is the flux density, and $(\mu_{en}/\rho)_j$ is the mass energy-absorption coefficient of air, which is given in Table 1[13], and G_V is a constant. The value of G_V amounts to 577 for the units of nGy·h^{-1}, MeV, cm^{-2}·s^{-1}·MeV^{-1}, and cm^2·g^{-1}, respectively.

The other is from conversion factors evaluated by Beck et al.[10] for uniformly distributed natural radionuclides in the soil, i.e.,

$$D_{CF} = 13.0C_K + 5.4C_U + 2.7C_{Th}, \qquad (13)$$

where, C_K(%), C_U(ppm) and C_{Th}(ppm) are the respective concentrations of K, U and Th in the soil.

The term D_{SI}/D_{CF} in Fig. 4 represents the dose rate ratio. For the natural environment, the case, D_{SI}/D_{CF} =1, results in the most probable concentrations of the three nuclides.

When there is a man-made source in the environment, we can estimate the additional contribution from the value of $D_{SI}-D_{CF}$. Figure 5 shows an example of discriminating a very weak contribution of ^{137}Cs from natural component.

As far as the dose rate evaluation is concerned,

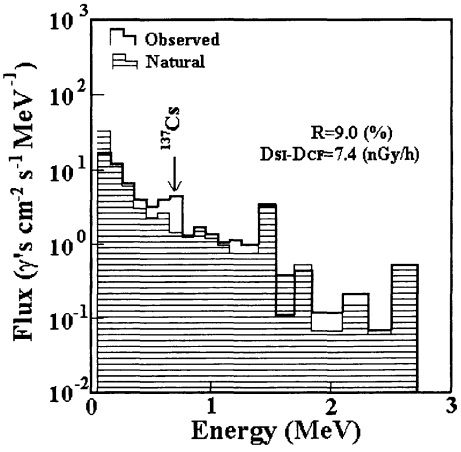

Fig. 5 Discrimination between the natural component and the weak gamma rays emitted from ^{137}Cs.

there is no big change due to updating the standard response matrix and flux density data. However, for the estimation of K, U and Th concentrations, considerable improvement is expected. Furthermore, the estimation of U concentration has so far been performed by using the energy bin 16 alone[2], while we used the two energy bins 16 and 18 in this study. This change may affect the evaluated results slightly. A general description on the accuracy of the DEF method will be published in the near future.

References

1) Minato, S. and Kawano, M.: Evaluation of exposure due to terrestrial gamma-radiation by response matrix method, *J. Nucl. Sci. Technol.*, **7**, 401-406 (1970)
2) e.g., Minato, S.: Analysis of environmental gamma ray pulse height distribution by response matrix method, *JCAC*, No.32, 2-13 (1998), in Japanese
3) Monahan, J. E.: "Scintillation Spectroscopy of gamma-Radiation Vol.1",(Shafroth, S. M. Ed.) Chapter VIII, Gordon and Breach Science Publishers (1967)
4) Minato, S.: Terrestrial gamma-radiation field in natural environment, *J. Nucl. Sci. Technol.*, **8**, 342-347 (1971)
5) Matsuda, H., Furukawa, S., Kaminishi, T. and Minato, S.: A new method for evaluating weak leakage gamma-ray dose using a 3"ϕ x 3" NaI(Tl) scintillation spectrometer (I) Principle of background estimation method, *Reports of the Government Industrial*

Research Institute, Nagoya, **31**, 132-146 (1982), in Japanese

6) Minato, S., Takamori, K. and Ikebe, Y.: Indoor cosmic-ray dosimetry by means of a 3"ϕ spherical NaI(Tl) scintillation counter, *Reports of the Government Industrial Research Institute, Nagoya*, **32**, 14-25 (1983), in Japanese

7) Nagaoka, T., Saito, K. and Moriuchi, S.: Ground level cosmic ray pulse height spectrum of a 7.5 cm diameter spherical NaI(Tl) scintillation detector for energy region below 5 MeV, *Hoken Butsuri*, **23**, 201-207 (1988), in Japanese

8) Minato, S.: Analysis of the variation of environmental g radiation during rainfall, *Reports of the Government Industrial Research Institute, Nagoya*, **26**, 190-202 (1977), in Japanese

9) Beck, H. L.: The absolute intensities of gamma rays from the decay of ^{238}U and ^{232}Th, Health and Safety Laboratory Report HASL-262, U.S. Atomic Energy Commission, New York, NY 10014 (1972)

10) Beck, H. L., DeCampo, J. and Gogolak, C.: In-situ Ge(Li) and NaI(Tl) gamma-ray spectrometry, Health and Safety Laboratory Report HASL-258, U.S. Atomic Energy Commission, New York, NY 10014 (1972)

11) Berger, M. J. and Seltzer, S. M.: Response functions for sodium iodide scintillation detectors, *Nucl. Instrum. Meth.*, **104**, 317-332 (1972)

12) Minato, S. and Matsuda, H. : A simple method of modifying a response matrix for a NaI(Tl) scintillator matching with its resolution, *Reports of the Government Industrial Research Institute, Nagoya*, **43**, 317-334 (1994), in Japanese

13) Hubbell, J. H.: Photon cross sections, attenuation coefficients, and energy absorption coefficients from 10 keV to 100 GeV, National Bureau of Standards Report NSRDS-NBS 29, Washington D.C., 20402 (1969)